

Naphthalene exposure decreases reduced glutathione in male Wistar rats

Ige Olaoye¹, Ayodeji Awotula¹, Babatunde Oso¹, Olubukola Agboola¹,
Godswill Akhigbe², Tuminimu Olaoye¹

¹ Department of Biochemistry, McPherson University, Seriki Sotayo, Nigeria

² Department of Chemical Sciences, McPherson University, Seriki Sotayo, Nigeria
akhigbegodswill@gmail.com

ABSTRACT

The study assessed the probable effects of naphthalene exposure through *in vivo* and *in silico* approaches. The *in vivo* assessment was carried on the glutathione (GSH) level in twenty-four Wistar Rats in two main groups based on different exposure times (2 and 4 h). These two groups were sub-grouped into three groups of four rats per group for 14 days. The *in silico* study was done on naphthalene and its metabolite towards glutamate-cysteine ligase (GCL) (the regulatory enzyme in GSH synthetic pathway) and glutathione reductase (GR). The result revealed that for 2 h of naphthalene exposure, the lower dose (0.75 g/m³) showed the highest reduced GSH level (93.50 ± 4.33 μmol/L) while the higher dose (1.50 g/m³) showed the least reduced GSH level (59.25 ± 7.57 μmol/L). In almost similar pattern, the 4 h exposure of naphthalene at both doses depicted a significant reduction compared to the control. The molecular docking study substantiated with the dynamics study revealed that naphthalene and all its metabolites had better binding score than glutathione (4.63 ± 0.15 kcal/mol) towards GCL with a common interacting residues (Leu-62, Val-63, Arg-64 and Phe-96). However, 4-hydroxychalcone had the best binding score (7.43 ± 0.58 kcal/mol) towards GR compared naphthalene and its metabolites. This study suggested that all naphthalene metabolites could possess more inhibitory potency than naphthalene towards GCL (except naphthalene epoxide) and GR.

Keywords: Naphthalene, Glutamate-cysteine ligase, Glutathione reductase, molecular docking

RESUMEN

Disminución de glutatión reducido en ratas Wistar machos tras la exposición a naftaleno. En el estudio se evaluó los posibles efectos de la exposición al naftaleno (GSH) mediante abordajes *in vivo* e *in silico*. En el estudio *in vivo* se evaluó los niveles de glutatión en 24 ratas Wistar, distribuidas en dos grupos principales a 2 y 4 h de exposición. Los grupos se subdividieron en tres subgrupos de 4 ratas cada uno, durante 14 días. En el estudio *in silico* se analizaron el naftaleno y sus metabolitos con respecto a la ligasa de glutamato-cisteína (GCL; enzima reguladora de la ruta sintética de GSH) y la glutatión reductasa (GR). Tras 2 h de exposición a naftaleno, la dosis menor (0.75 g/m³) mostró los mayores niveles de GSH reducido (93.50 ± 4.33 μmol/L), mientras que la dosis mayor (1.50 g/m³) los menores niveles (59.25 ± 7.57 μmol/L). Con un patrón casi similar, la exposición a ambas dosis de naftaleno durante 4 h provocó una disminución significativa en comparación con el control. El estudio de acoplamiento molecular complementado con el análisis de dinámica molecular reveló que el naftaleno y sus metabolitos tuvieron un mejor coeficiente de unión hacia la GCL que el GSH (4.63 ± 0.15 kcal/mol), al interactuar con aminoácidos similares (Leu-62, Val-63, Arg-64 and Phe-96). Sin embargo, la 4-hidroxichalcona mostró el mejor coeficiente de unión con la GR. El estudio sugirió que los metabolitos del naftaleno pueden mostrar una potencia inhibidora mayor que el naftaleno hacia la GCL (con excepción del epóxido de naftaleno) y la GR.

Palabras clave: naftaleno, ligasa de glutamato-cisteína, reductasa de glutatión, acoplamiento molecular

How to cite (Vancouver style):

Olaoye I, Awotula A, Oso B, Agboola O, Akhigbe G, Olaoye T. Naphthalene exposure decreases reduced glutathione in male Wistar rats. *Biotecnol Apl.* 2022;39(1):1201-10.

Introduction

The exposure of humans to the xenobiotics always poses unclear biological interactions. Toxicity is the potential of a substance to produce an adverse response upon a sufficient concentration in the body; such synthesized substances are called toxicants, man-made toxic substances or their products, capable of producing a deleterious effect. These harmful exogenous substances include but are not limited to mercury, lead, cyanide, asbestos, per-and polyfluoroalkyl substances and polychlorinated Biphenyl, among others [1]. The presence of these exogenous chemicals such as polycyclic aromatic hydrocarbons (PAHs) as well as their endogenous metabolic products in the human body might produce highly reactive species. Those reactive species, possessing unpaired electron, may be free radicals such as Reactive Oxygen Species

(ROS) and Reactive Nitrogen Species, which are both unstable and reactive [2]. Furthermore, these reactive species are harmful by causing the oxidation of macromolecules, which leads to tissue damage and cell death. Despite, they show some beneficial effects in certain physiological processes, such as fighting infectious agent by neutrophils [3-5].

PAHs are group of chemicals containing two or more condensed aromatic rings known as environmental toxicants [6-8] in which carcinogenicity is their most toxicity potential [9]. PAHs with at most four rings are known as light PAHs, and those with more than four rings are heavy PAHs. Kuppusamy *et al.* [10] and Li *et al.* [11] reported relative stability and toxic effect of heavy PAHs to light PAHs. Naphthalene, a two aromatic ring is the simplest PAH [12].

1. EPA. Chemicals and Toxics. 2021(cited Jan 20, 2021). Available from: <https://www.epa.gov/environmental-topics/chemicals-and-toxics-topics>.

2. Veskoukis AS, Tsatsakis AM, Kouretas D. Dietary oxidative stress and antioxidant defense with an emphasis on plant active administration. *Cell Stress and Chaperones*. 2012;17:11-21.

3. Valko M, Izakovic M, Mazur M, Rhodes CJ, Telser J. Role of oxygen radicals in DNA damage and cancer incidence. *Mol Cell Biochem*. 2004;266:37-56

4. Valko M, Leibfritz D, Moncol J, Cronin MT, Mazur M, Telser J. Free radicals and antioxidants in normal physiological functions and human disease. *Int J Biochem Cell Biol*. 2007;39(1):44-84.



Publicación libre de costo
para el autor
No article processing charges

The toxicity of Naphthalene is due to reactive species generation arising from the bio-activation of Naphthalene to highly cytotoxic epoxide such as 1R, 2S-naphthalene oxide by cytochrome P450s: CYP2F2 and CYP2F4 respectively [13]. A report has shown that naphthalene induced hepatic damage in male Wistar rats via oxidative stress [14]. In fact, Naphthalene toxicity is sex dependent as seen in Carratt *et al.* [15], reporting that the increase in susceptibility to cellular damage by Naphthalene was observed in female mice.

To put an end to this inevitable side effect for aerobic life, aerobic organisms utilize a defensive mechanism known as antioxidant system [16]. Antioxidants are substances that delay, prevent or remove oxidative damage from a target molecule. Antioxidants, especially those derived from natural sources and the non-enzymatic metabolites such as polyphenols, vitamins, glutathione (GSH), have potential applications in prevention and/or cure of human disease [17, 18]. GSH, a tripeptide, is the most important metabolite antioxidant and the most abundant low-molecular weight thiol-containing compound in biological fluids and tissues of mammals [2]. GSH is in dynamic equilibrium with oxidized GSH (GSSG) and contributes to xenobiotic detoxification. This phenomenon leads to the production of GSSG from GSH, thereby protecting the macromolecules from oxidative damage. The nonstop availability of reduced GSH, due to its constant conversion to GSSG for quenching the reactive species, results from naphthalene and/or its metabolites. Thus, replenishing GSH pool is favored through the continuous reduction of the GSSG by GSH reductase (GR) in the presence of NADPH.

Therefore, this work was aimed to investigate the conversion rate of GSH to GSSG upon the exposure of male Wistar rats to Naphthalene, and the molecular docking of naphthalene and its metabolites towards GR reduction rate.

Materials and methods

Reagents and animals

Naphthalene was purchased from Loba Chemie laboratory reagents and fine chemicals, India. Eighteen 2 to 3 months old, male Wistar rats, weighing 175-250 g, were purchased from the Animal Housing Facility of the Department of Physiology, University of Ibadan, Oyo State, Nigeria. They were used due to phylogenetics relationship of mammals order. Animals were kept in ventilated cages at room temperature (28-30 °C) and maintained on normal laboratory chow (Ladokun Feeds Ibadan, Oyo State, Nigeria) and water *ad libitum*. All experimental procedures were carried out in accordance with the NIH Guidelines for the care and use of Laboratory Animals. The animals were allowed to acclimatize for two weeks before the experiment.

Methods

Animal grouping and GSH assay for *in vivo* study

Eighteen Wistar were randomly divided into six groups of four rats each. Group 1 (Control 1) and group 2 (Control 2) rats were given food and water only. Group 3 (N1) and Group 5 (N3) rats were exposed

to Naphthalene vapor at 0.75 mg/m³ for 2 or 4 h, respectively; Group 4 (N2) and Group 6 (N4) rats were exposed to Naphthalene vapor at 1.5 mg/m³ for 2 or 4 h, respectively. The animals were given standard laboratory chow and water *ad libitum*, except for the time when they were exposed to Naphthalene vapor for 14 days. The rats were sacrificed 24 h after the last hour of Naphthalene exposure and an overnight fast. Blood samples were collected into plain bottle and centrifuged at 650 g for 5 min and the serum separated from the blood cells. Sera were kept frozen at -20 °C until GSH analysis.

The reduced GSH content in serum was quantified as non-protein sulfhydryls according to the Sedlak and Lindsay [19] method. Briefly 1.0 mL of the sample was deproteinized by the addition of 0.1 mL of 10 % trichloroacetic acid (TCA) and centrifuged at 650 × g for 5 min. Exactly 0.5 mL of supernatant was treated with 0.5 mL of Ellman's reagent (19.8 mg of 5,5'-dithiobis (2-nitrobenzoic acid; DTNB) in 100 mL of 0.1 % sodium nitrate) and 3.0 mL of phosphate buffer (0.2 M, pH 8.0). The absorbance was read against the reagent blank at 412 nm.

Glutathione concentration was calculated by the following formula:

$$\text{GSH concentration } (\mu\text{mol/L}) = \Delta A \times \frac{TV}{\epsilon} \times SV$$

Where: ΔA is the change in absorbance; TV the total volume, SV the sample volume and ε the molar extinction (1.34 × 10⁴ M⁻¹ cm⁻¹).

In silico study

In addition to the *in vivo* GSH biochemical assay, an *in silico* study was preformed to predict the binding affinity of GCL and GR active sites to naphthalene and its metabolites, as well as GSH (known inhibitor for glutamate-cysteine ligase) and 4-hydroxylchalcone (known inhibitor for GR). The selected naphthalene metabolites are reported molecules with high potentials of toxic effects. The protein and ligands were converted to the dockable pdbqt format using Autodock tools. The crystal structure was prepared by removing existing ligands and water molecules. Pdbqt format of the protein, as well as those of the ligands, was dragged into their respective columns and the software was run. Docking of the ligands to the protein target and the binding scores determination was carried out using PyRx-Python Prescription 0.8 (The Scripps Research Institute) [20]. The dimensions were set as grid center: x = 7.6311, y = 13.8268, z = 100.8810 and size: x = 65.0915, y = 67.9727, z = 40.8427 for GCL, and center: x = 70.4165, y = 51.3045, z = 18.7114 and size: x = 73.7137, y = 56.1634, z = 65.0941 for GR PDB code: 1GRA. The binding score of naphthalene and its selected metabolites are compared to the binding score of 4-Hydroxylchalcone.

Ligands and protein preparation

Three-dimensional (3D) SDF structures were retrieved from PubChem database (www.pubchem.ncbi.nlm.nih.gov) [21] for Naphthalene (CID: 931), its metabolites (such as 1,2-Naphthoquinone CID: 10667, 1-methylnaphthalene CID: 7002, 1-Nitro-naphthalene CID: 6349 and Naphthalene epoxide

5. Sabale V, Kunjwani H, Sabale P. Formulation and *in vitro* evaluation of the topical antiageing preparation of the fruit of Benincasa hispida. J Ayurveda Integr Med. 2011;2(3):124-8.

6. Slezakova K, Pires JCM, Castro D, Alvim-Ferraz MDCM, Delerue-Matos C, Morais S, et al. PAH air pollution at a Portuguese urban area: Carcinogenic risks and sources identification. Environ Sci Pollut Res. 2013;20:3932-45.

7. Nakata H, Uehara K, Goto Y, Fukumura M, Shimasaki H, Takikawa K. Polycyclic aromatic hydrocarbons in oysters and sediments from the Yatsushiro Sea, Japan: Comparison of potential risks among PAHs, dioxins and dioxin-like compounds in benthic organisms. Ecotoxicol Environ Saf. 2014;99:61-8.

8. Honda M, Suzuki N. Toxicities of Polycyclic Aromatic Hydrocarbons for Aquatic Animals Int. J. Environ. Res. Public Health. 2020;17:1363.

9. Devi NL, Yadav IC, Shihua Q, Dan Y, Zhang G, Raha P. Environmental carcinogenic polycyclic aromatic hydrocarbons in soil from Himalayas, India: Implications for spatial distribution, sources apportionment and risk assessment. Chemosphere. 2016;144:493-502.

10. Kuppasamy S, Thavamani P, Megharaj M, Naidu R. Biodegradation of polycyclic aromatic hydrocarbons (PAHs) by novel bacterial consortia tolerant to diverse physical settings - Assessments in liquid- and slurry-phase systems. Int Biodeter and Biodegradation. 2016;108:149-57.

11. Li PH, Wang Y, Li YH, Wai KM, Li HL, Tong L. Gas-particle partitioning and precipitation scavenging of polycyclic aromatic hydrocarbons (PAHs) in the free troposphere in southern China. Atmospheric Environ. 2016;128:165-74.

12. Parales RE, Ju KS. Rieske-type dioxygenases: Key enzymes in the degradation of aromatic hydrocarbons. In: Murray Moo-Young, Comprehensive Biotechnology (Second Edition). New York: Academic Press; 2016. p. 115-34.

13. Baldwin RM, Jewell WT, Fanucchi MV, Plopper CG, Buckpitt AR. Comparison of pulmonary/nasal CYP2F expression levels in rodents and rhesus macaque. J Pharmacol Exp Ther. 2004;309:127-36.

14. Kushwah DS, Salman MT, Singh P, Verma VK, Ahmad A. Protective effects of 14.nolic extract of *Nigella sativa* seed in paracetamol induced acute hepatotoxicity *in vivo*. Pak J Biol Sci. 2014;17(4):517-22.

15. Carratt S, Morin D, Buckpitt AR, Edwards PC, Vas Winkle LS. Naphthalene cytotoxicity in microsomal epoxide hydrolase deficient mice. Toxicology Lett. 2016;246:35-41.

16. Halliwell B, Gutteridge JMC. Free radicals in biology and medicine, 4th edn. Oxford: Clarendon; 2007.

17. Sies H. Antioxidants in Disease, Mechanisms and Therapy. New York: Academic Press; 1996.

18. Nie G, Cao Y, Zhao B. Protective effects of green tea polyphenols and their major component, (-)-epigallocatechin-3-gallate (EGCG), on 6-hydroxydopamine-induced apoptosis in PC12 cells. Redox Report. 2002;7:171-7.

CID: 108063), GSH (CID: 124886), a known GCL inhibitor and 4-Hydroxychalcone (CID: 5282361), a known GR inhibitor. The rat primary sequence of GCL with UniProtKD ID: P48508 was retrieved from UniProt database (<https://www.uniprot.org/>) [22]. The obtained primary sequence was used in the prediction of the secondary structure of GCL using the SOPMA webserver (https://npsa-prabi.ibcp.fr/cgi-bin/npsa_automat.pl?page=NPSA/npsa_sopma.html) [23] while the swiss model webserver (<https://swissmodel.expasy.org/interactive/>) was used for the modelling of the GCL tertiary structure [24]. The foreseen GCL model was refined once through the GalaxyRefine web server to improve the quality of the protein (<http://galaxy.seoklab.org/cgi-bin/submit.cgi?type=REFINE2>) [25]. The online PROCHECK webserver (<https://saves.mbi.ucla.edu/>) [26, 27] and Qualitative Model Energy Analysis (QMEAN) Swiss Model server (<https://swissmodel.expasy.org/qmean/>) [28] were used for the structural characterization of the modeled GCL via the Ramachandran plot and QMEAN Version 4.1.0 respectively. Moreover, the GCL 3D structure was validated by ligand-binding sites analysis using COFACTOR (<https://zhanglab.cmb.med.umich.edu/COFACTOR/>) [29]. The three-dimensional (3D) X-Ray crystallography solution structure of GR was downloaded from the RCSB protein data bank (<http://www.rcsb.org>) [30].

Molecular dynamics simulations

The molecular dynamics simulations assessment was performed using CABS-flex server (<http://biocomp.chem.uw.edu.pl/CABSflex2>) [31] in order to investigate the conformational stability of the protein-ligand interactions, based on root mean square fluctuation (RMSF) value. Complexes of GCL and GR were loaded to the CABSflex server in default settings for analysis of the flexibility of the complexes.

Statistical analysis

The results obtained were expressed as mean \pm standard deviation of three determinations and analyzed using one-way analysis of variance (ANOVA) for mean differences between different doses followed by Duncan post hoc correlation (significant differences for $p < 0.05$).

Results and discussion

The metabolism of most environmental toxicants such as Naphthalene involves the biotransformation in a series of biochemical reactions from lipid-soluble substance to water soluble metabolites for easy excretion [32]. Here, Naphthalene is bio-activated by CYP450 to toxic quinones and reactive epoxide metabolites when accumulated. However, Buckpitt *et al.* [33] reported that the conjugation of these metabolites by reduced GSH produced soluble non-toxic products. Similarly, Greene *et al.*, West *et al.* and Plopper *et al.* [34-36] documented their findings on the critical roles of GSH towards the prevention of naphthalene toxicity.

It is evidenced from table 1 that reduced GSH, at both doses of Naphthalene exposure tested, was significantly different ($p < 0.05$) from the control (unexposed subjects). In the two hours of Naphthalene exposure, the lower dose (0.75 g/m³) showed the highest

Table 1. Antioxidant status of apparently healthy rats exposed to naphthalene for 2 and 4 h

Naphthalene concentration (g/m ³)	GSH concentration (μmol/L)	
	2 h	4 h
0	61.00 \pm 6.93a	148.00 \pm 8.00a
0.75	93.50 \pm 4.33b	50.25 \pm 10.13b
1.50	59.25 \pm 7.57c	9.25 \pm 1.25c

* ANOVA followed by Duncan multiple range test for correlation analysis. Different letters stand for statistically significant differences ($p < 0.05$).

level of reduced GSH (93.50 \pm 4.33 μmol/L) followed by the control (61.00 \pm 6.93 μmol/L), while the higher dose (1.50 g/m³) showed the least reduced GSH (59.25 \pm 7.57 μmol/L). This result suggests that the high exposure to Naphthalene may not be toxic due to oxidative stress but cysteine deficiency [37]. Conversely, the result obtained at 4 h of Naphthalene exposure depicted a dose-dependent drastic reduction of reduced GSH compared to the control. This result suggests that longer times of naphthalene exposure depleted the reduced GSH level. It confirms reports by Phimister *et al.* [38], on the insufficient GSH supply from the liver preventing the ameliorating effect of GSH on Naphthalene induced toxicity. Moreover, the GSH result coincides with Stohs *et al.* [39], on the depletion of reduced GSH in Naphthalene induced toxicity. The significant decrease in GSH level in the serum could be due to excessive free radical generated arose from the binding of Naphthalene to various sulfhydryls existing in the system [40].

To substantiate toxicity effects, molecular docking was performed to investigate Naphthalene and its metabolites interaction toward glutamate-cysteine ligase (GCL) and GR in the assessment of GSH level. The molecular docking revealed that Naphthalene and all its metabolites showed better binding score (-4.63 ± 0.15 kcal/mol) than GSH (a known feedback inhibitor [41]) (Table 2). This high binding score could be due to high number of pi-pi stacked interactions between the heteroaromatic rings of the ligands as well as few conventional hydrogen bonds formation with the interacting residues [42, 43].

Despite, the GSH-GCL interaction had the highest number of conventional hydrogen bond formation as compared to Naphthalene and its metabolites, that could contribute to its high binding score [44]. The lack of interaction with the common interacting residues (Leu-62, Val-63, Arg-64 and Phe-96) as seen in Naphthalene and its metabolites, except 1,2 naphthoquinone that interacted with two common interacting

Table 2. Binding scores of naphthalene, 1,2-naphthoquinone, 1-methylnaphthalene, 1-nitronaphthalene, 1,4-naphthoquinone and naphthalene epoxide toward glutamate-cysteine ligase

Compounds/CID	Binding score (kcal/mol)	Amino acid residues interaction
Naphthalene, 931	-6.00 \pm 0.00a	Leu-62, Val-63, Arg-64, Phe-96
1,2-naphthoquinone, 10667	-6.17 \pm 0.21a	Leu-62, Phe-96
1-methylnaphthalene, 7002	-6.37 \pm 0.06b	Leu-62, Val-63, Arg-64, Phe-96, Val-98
1-nitronaphthalene, 6849	-6.13 \pm 0.06a	Leu-62, Val-63, Arg-64, Glu-65, Phe-96, Val-98
1,4-naphthoquinone, 8530	-6.10 \pm 0.00a	Leu-62, Val-63, Arg-64, Phe-96
Naphthalene epoxide, 108063	-5.67 \pm 0.12c	Leu-62, Val-63, Arg-64, Phe-96
Glutathione, 124886	-4.63 \pm 0.15d	Arg-30, Arg-32, Ser-55, Gln-240

* ANOVA followed by Duncan multiple range test for correlation analysis. Different letters stand for statistically significant differences ($p < 0.05$).

19. Sedlak J, Lindsay RH. Estimation of total, protein-bound, and non-protein sulfhydryl groups in tissues with Ellman's reagent. *Anal Biochem.* 1958;25(1):192-205.

20. Trott O, Olson AJ. AutoDock Vina: Improving the speed and accuracy of docking with a new scoring function, efficient optimization and multithreading. *J Comp Chem.* 2010;31(2):455-61.

21. Kim S, Chen J, Cheng T, Gindulyte A, He J, He S, *et al.* PubChem 2019 update: improved access to chemical data. *Nucleic Acids Res.* 2019;47(D1):D1102-9.

22. The UniProt Consortium. UniProt: the universal protein knowledgebase in 2021. *Nucleic Acids Res.* 2021;49(D1): D480-9.

23. Combet C, Blanchet C, Geourjon C, Deléage G. NPS@: network protein sequence analysis. *Trends Biochem Sci.* 2000;25(3):147-50.

24. Waterhouse A, Bertoni M, Bienert S, Studer G, Tauriello G, Gumienny R, *et al.* SWISS-MODEL: homology modelling of protein structures and complexes. *Nucleic Acids Res.* 2018;46(W1):W296-303.

25. Lee GR, Won J, Heo L, Seok C. GalaxyRefine2: simultaneous refinement of inaccurate local regions and overall protein structure. *Nucleic Acids Res.* 2019;47(W1):W451-5.

26. Laskowski RA, MacArthur MW, Moss DS, Thornton JM. PROCHECK: a program to check the stereochemical quality of protein structures. *J Appl Crystal.* 1993;26(2):283-91.

27. Laskowski RA, Rullmann JA, MacArthur MW, Kaptein R, Thornton JM. AQUA and PROCHECK-NMR: programs for checking the quality of protein structures solved by NMR. *J Biomol NMR.* 1996;8(4):477-86.

28. Benkert P, Biasini M, Schwede T. Toward the estimation of the absolute quality of individual protein structure models. *Bioinformatics.* 2011;27(3):343-50.

residues (Leu-62 and Phe-96), could be responsible for the low binding score observed in GSH. Also, the result could suggest that these residues in the GCL as well as their respective position play a key role in the protein-ligand interaction.

Conversely, none of the compounds (Naphthalene and its metabolites) had better binding score than the inhibitor (4-hydroxychalcone; 7.43 ± 0.58 kcal/mol) (Table 3). This could be due to the high number of conventional hydrogen bond formation in 4-hydroxychalcone [44]. Nevertheless, all the metabolites of Naphthalene have better binding score than Naphthalene (-5.83 ± 0.12 kcal/mol) except 1,2-naphthoquinone (-5.80 ± 0.17 kcal/mol). Interestingly, as shown in figure 1A and B, all the ligands interacted with polar amino acid residues (Ser-51, Lys-53, Thr-57, Ser-177, Tyr-197, Arg-291, Asp-331, and Ser-471 except Ile-466) of GR via conventional hydrogen bond except naphthalene and 1-methylnaphthalene. Such interaction could be responsible to their high binding scores [45, 46] (Figures 2 and 3). Besides, all the ligands and 4-hydroxychalcone had a significant better binding score compared to Naphthalene except 1,2-naphthoquinone. This low binding score in 1,2-naphthoquinone, despite the presence of conventional hydrogen bond, may be due to unfavorable donor-donor interaction between GR and 1,2-naphthoquinone. Such unfavorable donor-donor interaction is responsible for the repulsive effect between GR and 1,2-naphthoquinone, by lowering the stability of the GR [47].

The results of molecular dynamics for the docked complexes together with GCL and GR wild-types are depicted in figures 3 and 4, respectively. These two proteins (GCL and GR) were considered for the *in silico* study due to the important roles placed in the availability of GSH. GCL is the regulatory enzyme in the GSH biosynthetic pathway, while GR catalyzes the reduction of oxidized GSH (GSSG) to GSH, to ensure its continuous availability in the system. All these revealed a significant reduction in the fluctuation of residues A133-A153 of GCL-ligand complexes (Naphthalene and its metabolites), while GSH showed no significant alteration in the residues when compared to GCL wild-type. This significant decrease within the A133-A153 region could reduce the flexibility of the protein, suggesting the increased binding scores observed in Naphthalene and its metabolites when compared to GSH [47].

Also, the GR wild-type dynamics results showed high fluidity within these two regions, 85-91 and 359-365. Meanwhile, the inhibitor (4-hydroxychalcone) with GR depicted an increase in the rigidity of GR than any of the ligands within these regions, suggesting that reduced 4-hydroxychalcone fluidity for the GR wild-type could be responsible for its inhibition property towards GR. This observation is in line with that observed by Zhang *et al.* [48], on the inhibitory potential of 4-hydroxychalcone on GR. Nevertheless, Naphthalene and its metabolites increase the fluidity of GR, except 1-methylnaphthalene and 1,4-naphthoquinone, with respective RSMF values 3.049 and 3.567 within this region (85-91 residues). Interestingly, complexes of Naphthalene and all its metabolites showed higher fluidity compared to 4-hydroxychalcone-GR complex.

Table 3. Binding scores of naphthalene, 1,2-naphthoquinone, 1-methylnaphthalene, 1-nitronaphthalene, 1,4-naphthoquinone, naphthalene epoxide, and 4-Hydroxychalcone with glutathione reductase

Compounds/CID	Binding score (kcal/mol)	Amino acid residues interaction
Naphthalene, 931	$-5.83 \pm 0.12d$	Lys-66, Tyr-197, Ile-198, Met-202
1,2-naphthoquinone, 10667	$-5.80 \pm 0.17d$	Lys-53, Gly-56, Thr-57
1-methylnaphthalene, 7002	$-6.30 \pm 0.06bc$	Lys-66, Tyr-197, Ile-198, Met-202
1-nitronaphthalene, 6849	$-6.50 \pm 0.58b$	Ser-30, Asp-331, Ala-342
1,4-naphthoquinone, 8530	$-6.57 \pm 0.12b$	Gly-62, Cys-63, Lys-66, Ser-177, Tyr-197, Ile-198, Met-202, Arg-291
Naphthalene epoxide, 108063	$-6.07 \pm 0.88cd$	Ser-51, His-129, Thr-156, Leu-298
4-Hydroxychalcone, 5282361	$-7.43 \pm 0.58a$	Ala-450, Phe-460, Thr-463, Ile-466, Ser-471, Val-475

* ANOVA followed by Duncan multiple range test for correlation analysis. Different letters stand for statistically significant differences ($p < 0.05$).

Figure 1. Molecular docking of glutamate-cysteine ligase. A) 2D-Molecular docking of glutamate-cysteine ligase towards: i) Naphthalene, ii) 1,2-naphthoquinone, iii) 1-methylnaphthalene, iv) 1-nitronaphthalene, v) 1,4-naphthoquinone, vi) Naphthalene epoxide, and vii) glutathione.

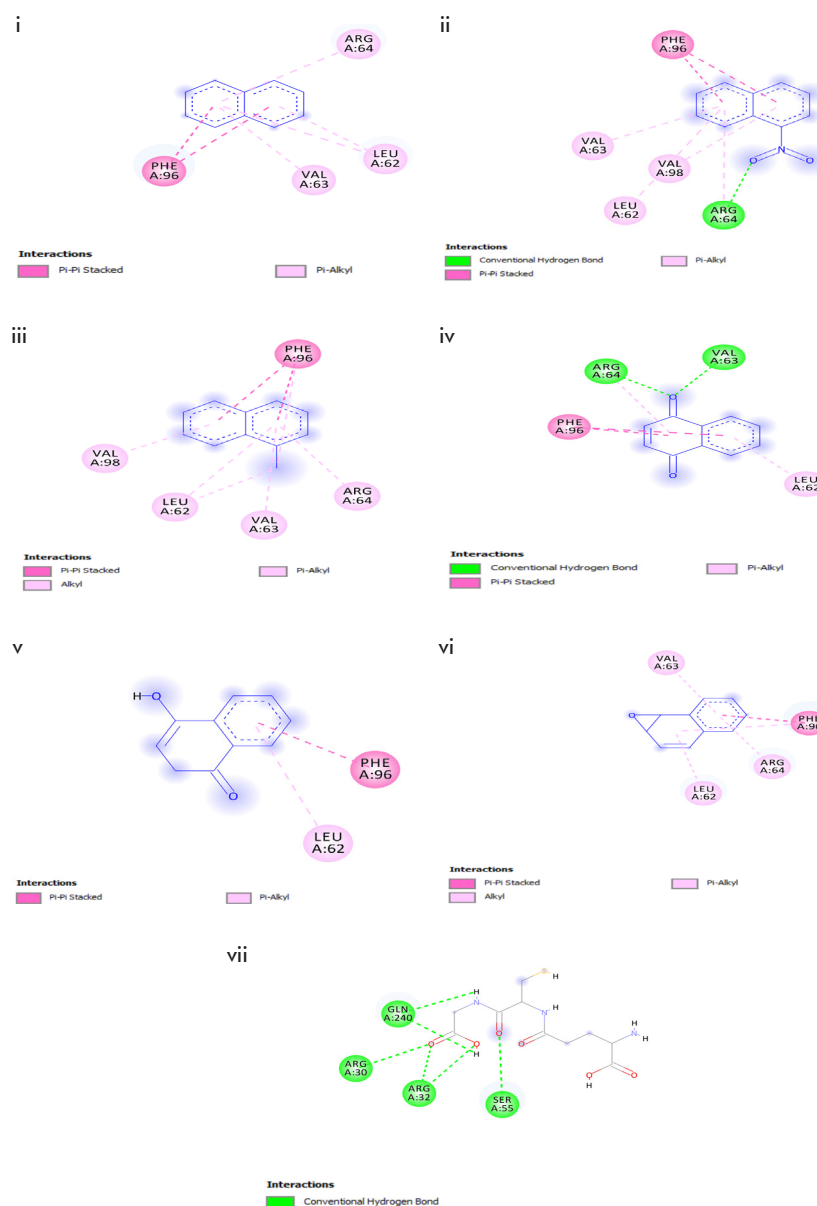


Figure 1 (continued). Molecular docking of glutamate-cysteine ligase. B) 3D-Molecular docking of glutamate-cysteine ligase towards: i) Naphthalene, ii) 1,2-naphthoquinone, iii) 1-methylnaphthalene, iv) 1-nitronaphthalene, v) 1,4-naphthoquinone, vi) Naphthalene epoxide, and (vii) glutathione.

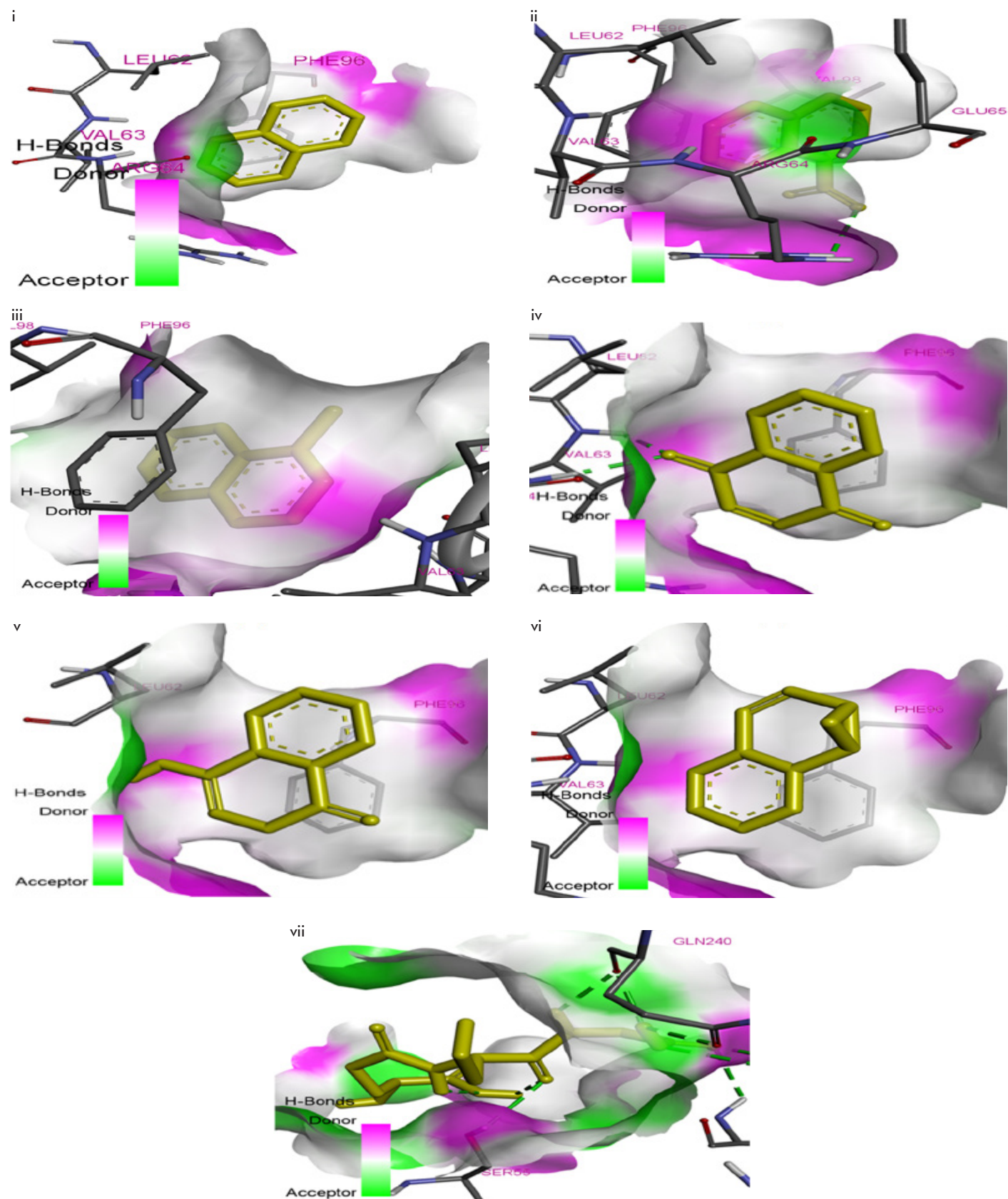


Figure 2. Molecular docking of glutathione reductase. 2D-Molecular docking of glutathione reductase. A) Docking towards: i) Naphthalene, ii) 1,2-naphthoquinone, iii) 1-methylnaphthalene, iv) 1-nitronaphthalene, v) 1,4-naphthoquinone, vi) Naphthalene epoxide, and vii) 4-hydroxychalcone.

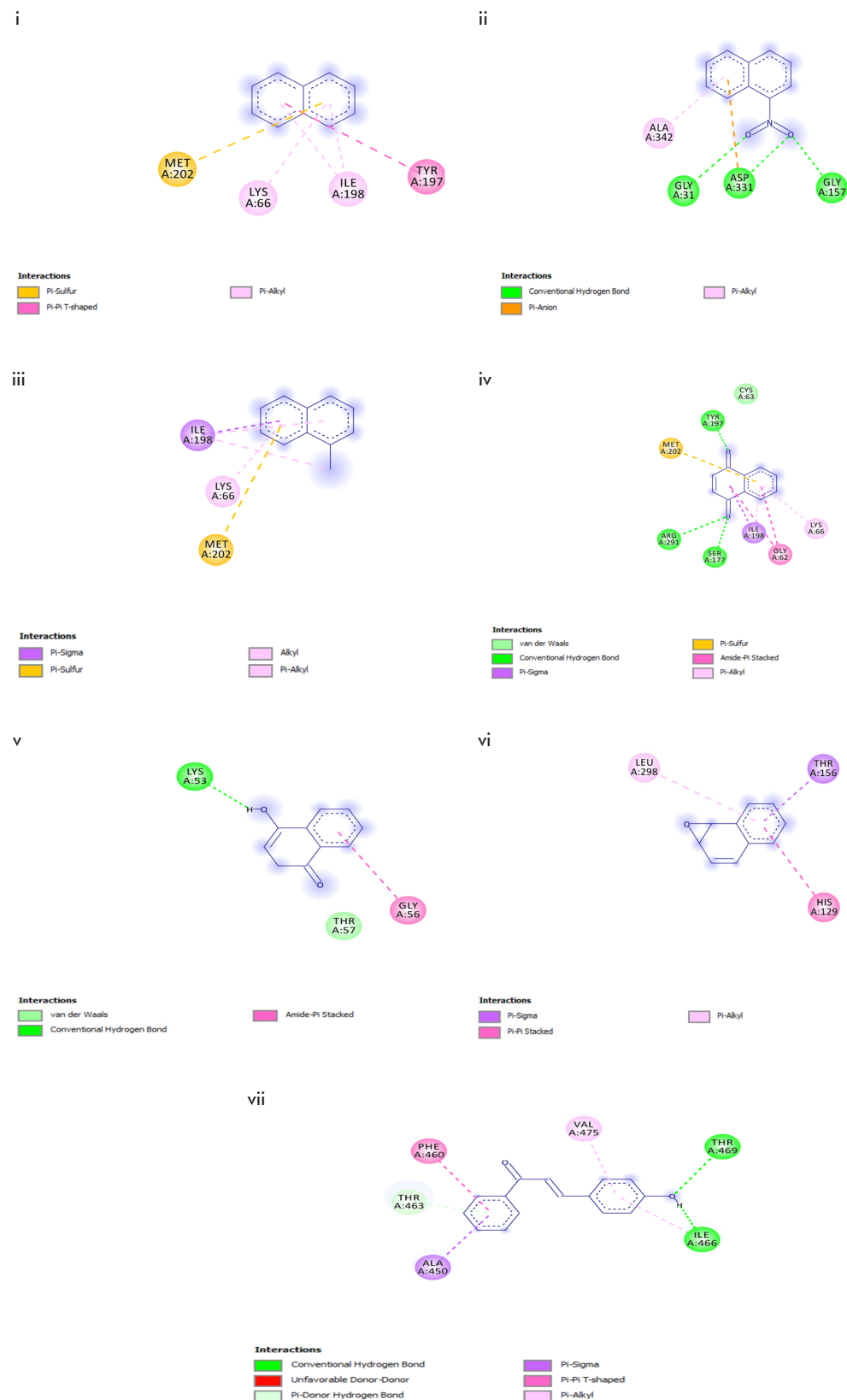


Figure 2 (continued). Molecular docking of glutathione reductase. B) 3D-Molecular docking of glutathione reductase. A) Docking towards: i) Naphthalene, ii) 1,2-naphthoquinone, iii) 1-methylnaphthalene, iv) 1-nitronaphthalene, v) 1,4-naphthoquinone, vi) Naphthalene epoxide, and vii) 4-hydroxychalcone.

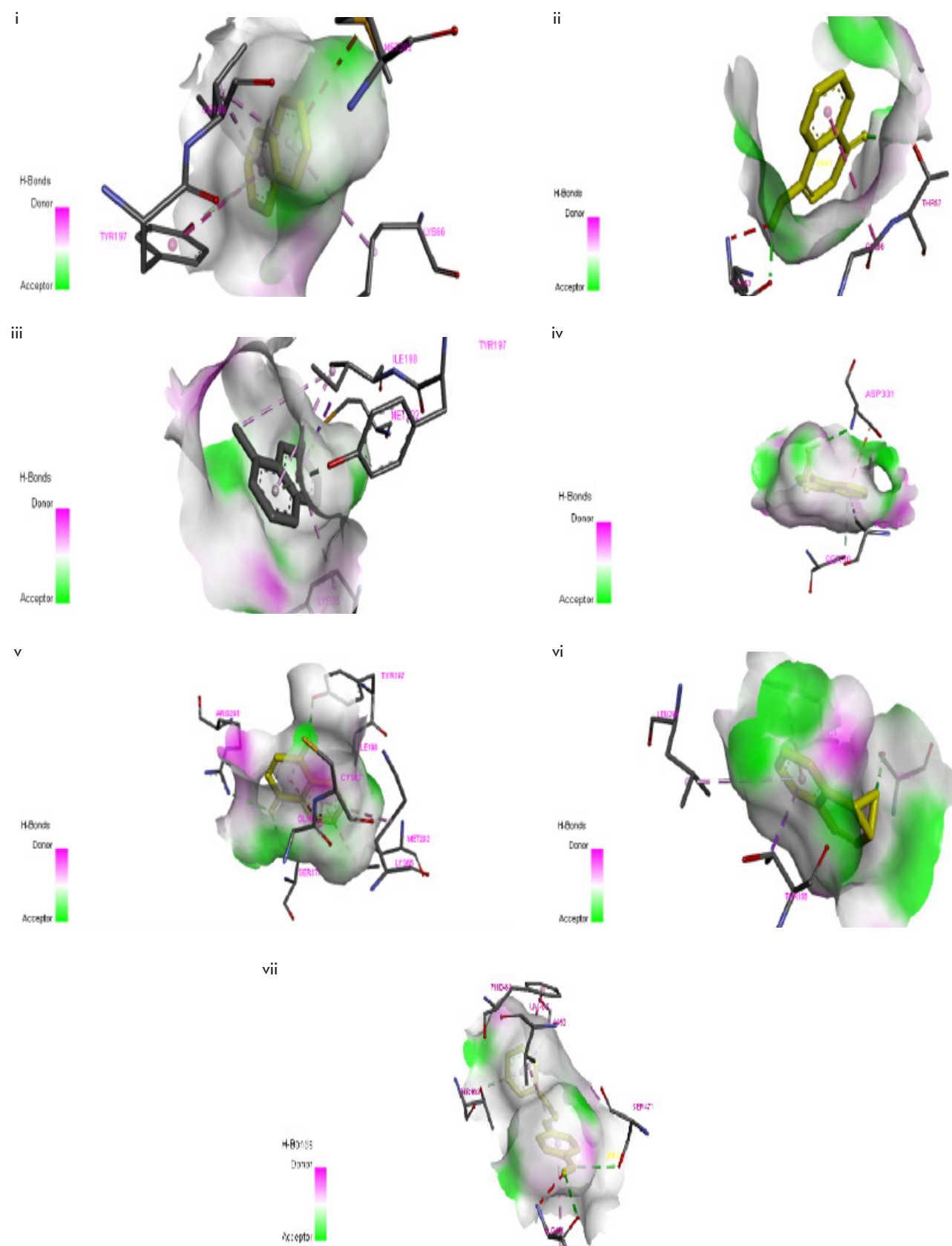


Figure 3. Molecular dynamics simulation showing the fluctuation plot. i) Naphthalene, ii) 1,2-naphthoquinone, iii) 1-methylnaphthalene, iv) 1-nitro-naphthalene, v) 1,4-naphthoquinone, vi) Naphthalene epoxide, and vii) glutathione on GCL and viii) GCL wild-type.

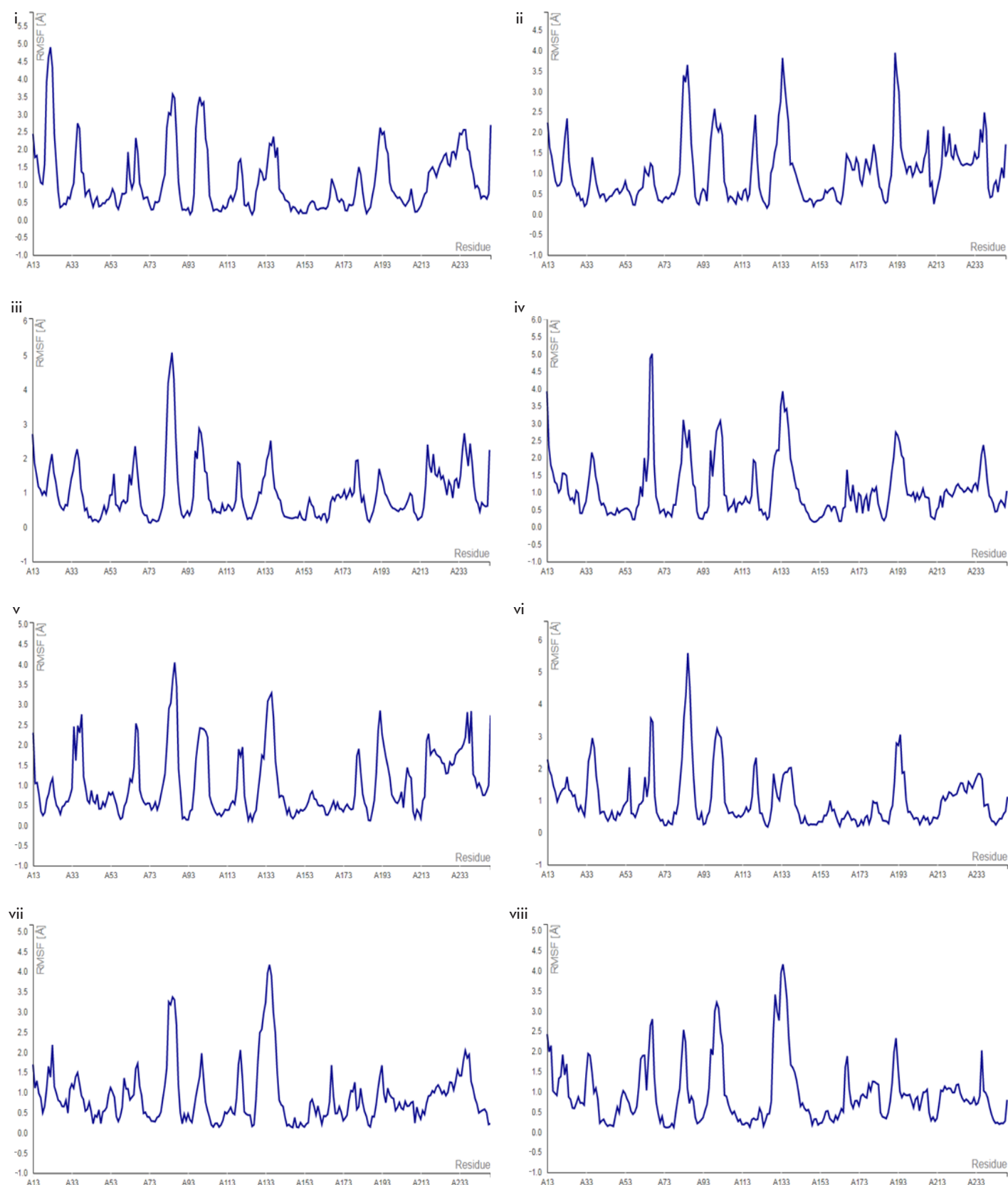
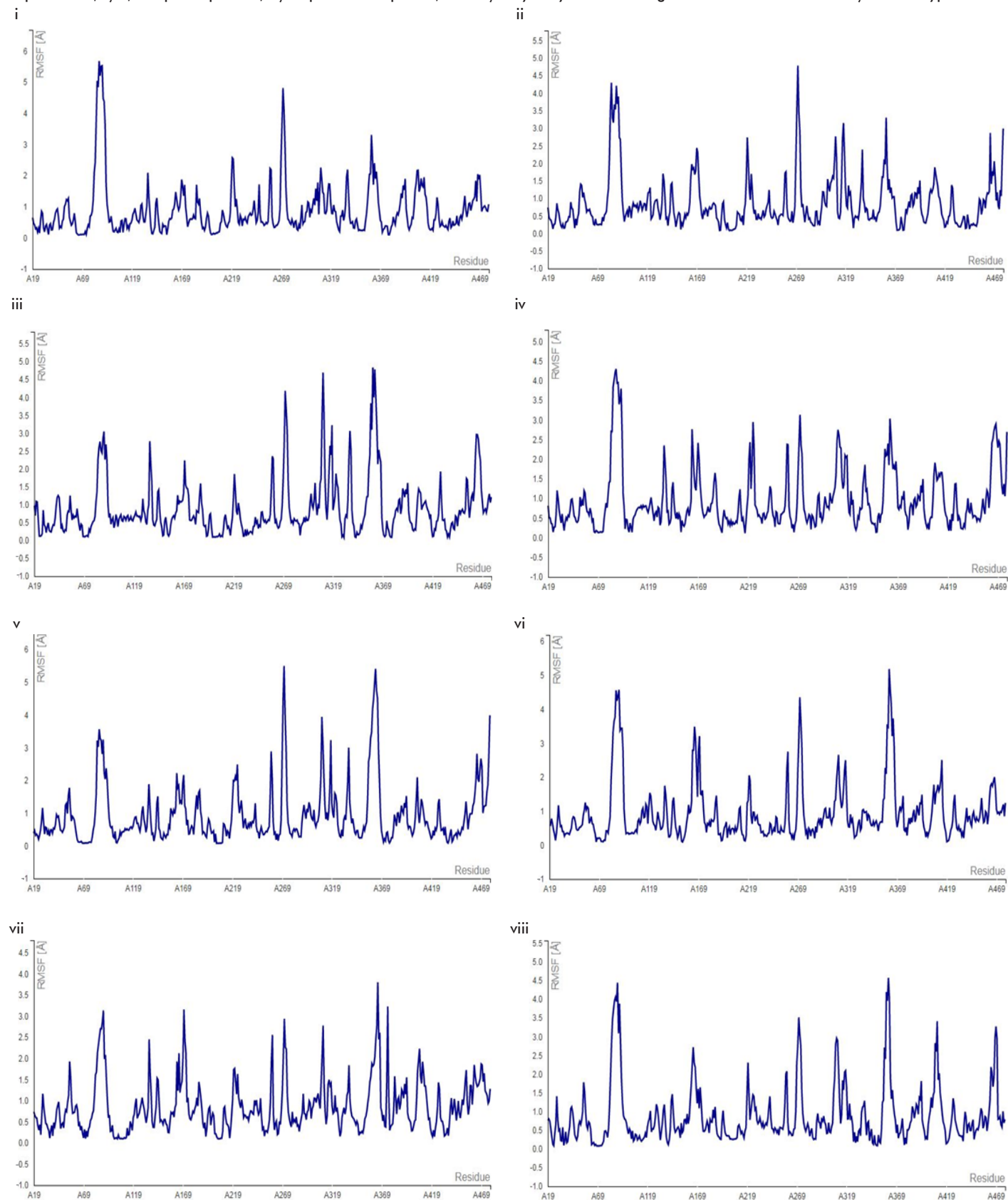


Figure 4. Molecular dynamics simulation showing the fluctuation plot. i) Naphthalene, ii) 1,2-naphthoquinone, iii) 1-methylnaphthalene, iv) 1-nitro-naphthalene, v) 1,4-naphthoquinone, vi) Naphthalene epoxide, and vii) 4-hydroxylchalcone on glutathione reductase and viii) GR wild-type.



It suggests lesser inhibitory potency and relevance of dynamicity of this region in GR towards inhibition. In a similar pattern, within the 359-365 residues' region, all complexes of ligands with GR showed higher fluidity than 4-hydroxychalcone-GR complex (except naphthalene, 1,2-naphthoquinone and 1-nitronaphthalene), suggesting that this variation in the GR fluidity in this region had a lower effect compared to the other region.

Conclusions

In summary, it can be concluded that Naphthalene exposure reduced the GSH level in a dose dependent

pattern at longer time of exposure. Also, Naphthalene showed lesser inhibitory effect as compared to its metabolites towards GCL (except Naphthalene epoxide), and GR and GSH showed lower inhibitory strength than Naphthalene and its metabolites. Meanwhile, 4-hydroxychalcone possessed higher inhibitory potential than Naphthalene and its metabolites according to its binding scores.

Conflicts of interest statement

The authors declare that there are no conflicts of interest.

29. Roy A, Yang J, Zhang Y. COFACTOR: an accurate comparative algorithm for structure-based protein function annotation. *Nucleic Acids Res.* 2012;40(W1):W471-7.

30. Berman HM, Westbrook J, Feng Z, Gilliland G, Bhat TN, Weissig H, et al. The Protein Data Bank. *Nucleic Acids Res.* 2000;28(1):235-42.

31. Kuriata A, Gierut AM, Oleniecki T, Cierny MP, Kolinski A, Kurcinski M, et al. CABS-flex 2.0: a web server for fast simulations of flexibility of protein structures. *Nucleic Acids Res.* 2018;46(W1):W338-43.

32. Parkinson A, Ogilvie BW. Biotransformation of xenobiotics. In: Klaassen CD (Ed.). Casarett & Doull's Toxicology the Basic Science of Poisons. 7th ed. New York: The McGraw Hill Companies, Inc.; 2008. p. 161-304.

33. Buckpitt, A, Boland B, Isbell M, Morin D, Shultz M, Baldwin R, et al. Naphthalene-induced respiratory tract toxicity: Metabolic mechanisms of toxicity. *Drug Metab Rev.* 2002; 34:791-820.

34. Greene JF, Zheng J, Grant DF, Hammock BD. Cytotoxicity of 1,2-epoxynaphthalene is correlated with protein binding and in situ glutathione depletion in cytochrome P4501A1 expressing Sf-21 cells. *Toxicol Sci.* 2000;53:352-60.

35. West JA, Buckpitt AR, Plopper CG. Elevated airway GSH resynthesis confers protection to Clara cells from naphthalene injury in mice

made tolerant by repeated exposures. *Environ Health Perspect.* 2000;118:647-52.

36. Plopper CG, Van Winkle LS, Fanucchi MV, Malburg SR, Nishio SJ, Chang A, et al. Early events in naphthalene-induced acute Clara cell toxicity. II. Comparison of glutathione depletion and histopathology by airway location. *Am J Respir Cell Mol Biol.* 2001;24:272-81.

37. Jones DP, Carlson JL, Mody VC, Cai J, Lynn MJ, Sternberg P. Redox state of glutathione in human plasma. *Free Radic Biol Med.* 2000;28(4):625-35.

38. Phimister AJ, Lee MG, Morin D, Buckpitt AR, Plopper CG. Glutathione depletion is a major determinant of inhaled naphthalene respiratory toxicity and naphthalene metabolism in mice. *Toxicol Sci.* 2004;82: 268-78.

39. Stohs SJ, Ohia S, Bagchi D. Naphthalene toxicity and antioxidant nutrients. *Toxicology.* 2002;180:97-105.

40. Vijayavel K, Anbuselvam C, Balasubramanian MP. Antioxidant effect of the marine algae *Chlorella vulgaris* against naphthalene-induced oxidative stress in the albino rats. *Mol Cell Biochem.* 2007;303:39-44.

41. Seelig GF, Simonsen RP, Meister A. Reversible dissociation of γ -glutamylcysteine synthetase into two subunits. *J Biol Chem.* 1984;259(15):9345-7.

42. Brylinski M. Aromatic interactions at the ligand-protein interface: Implications for the

development of docking scoring functions. *Chem Biol Drug Des.* 2018;91(2):380-90.

43. Arthur DE, Uzairu A. Molecular docking studies on the interaction of NCI anticancer analogues with human Phosphatidylinositol 4,5-bisphosphate 3-kinase catalytic subunit. *J King Saud University – Science.* 2019;31:1151-66.

44. Elokely KM, Doerksen RJ. Docking challenge: protein sampling and molecular docking performance. *J Chem Inf Model.* 2013;53(8):1934-45.

45. Chen D, Oezguen N, Urvil P, Ferguson C, Savidge TC. Regulation of protein-ligand binding affinity by hydrogen bond pairing. *Sci Adv.* 2016;2(3):1-17.

46. Olaoye I, Oso B, Aberuagba A. Molecular mechanisms of anti-inflammatory activities of the extracts of *Ocimum gratissimum* and *Thymus vulgaris*. *Avicenna J Med Biotechnol.* 2021;13(4):207-16.

47. Dhorajiwala TM, Halder ST, Samant L. Comparative in silico molecular docking analysis of L-Threonine-3-Dehydrogenase, a protein target against African trypanosomiasis using selected phytochemicals. *J Appl Biotechnol Rep.* 2019;6(3):101-8.

48. Zhang K, Yang EB, Tang WY, Wong KP, Mack P. Inhibition of glutathione reductase by plant polyphenols. *Biochem Pharmacol.* 1999;54(9):1047-53.

Received in October, 2021.

Accepted in December, 2021.